PCCP

PAPER

View Article Online
View Journal | View Issue

Cite this: *Phys. Chem. Chem. Phys.*, 2014, **16**, 4642

Probing the conformation and 2D-distribution of pyrene-terminated redox-labeled poly(ethylene glycol) chains end-adsorbed on HOPG using cyclic voltammetry and atomic force electrochemical microscopy†

Agnès Anne,* Mohamed Ali Bahri, Arnaud Chovin, Christophe Demaille* and Cécilia Taofifenua

Received 7th November 2013,
Accepted 9th January 2014

DOI: 10.1039/c3cp54720e

www.rsc.org/pccp

The present paper aims at illustrating how end-attachment of water-soluble flexible chains bearing a terminal functional group onto graphene-like surfaces has to be carefully tuned to ensure the proper positioning of the functional moiety with respect to the anchoring surface. The model experimental system considered here consists of a layer of poly(ethylene glycol) (PEG) chains, bearing an adsorbing pyrene foot and a ferrocene (Fc) redox functional head, self-assembled onto highly oriented pyrolytic graphite (HOPG). Cyclic voltammetry is used to accurately measure the chain coverage and gain insights into the microenvironment experienced by the Fc heads. Molecule-touching atomic force electrochemical microscopy (Mt/AFM-SECM) is used to simultaneously probe the chain conformation and the position of the Fc heads within the layer, and also to map the 2D-distribution of the chains over the surface. This multiscale electrochemical approach allows us to show that whereas Fc–PEG–pyrene readily self-assembles to form extremely homogeneous layers, the strongly hydrophobic nature of graphite planes results in a complex coverage-dependent structure of the PEG layer due to the interaction of the ferrocene label with the HOPG surface. It is shown that, even though pyrene is known to adsorb particularly strongly onto HOPG, the more weakly adsorbing terminal ferrocene can also act as the chain anchoring moiety especially at low coverage. However we show that beyond a critical coverage value the Fc–PEG–pyrene chains adopt an ideal "foot-on" end-attached conformation allowing the Fc head to explore a volume away from the surface solely limited by the PEG chain elasticity.

Introduction

Layers of end-attached poly(ethylene glycol) (PEG) chains are extensively used to alter the interfacial properties of many different materials in aqueous solutions.[1] These PEG layers notably display the unique properties of improving the biocompatibility of surfaces by preventing protein and microbial adsorption.[2,3] End-attached PEG chains have also been widely used to coat the surface of nano-objects, such as nanoparticles,[4,5] or carbon nanotubes,[6,7] in order to prevent particle aggregation, but also to render them suitable for bio-analytical applications, or for *in vivo*-applications such as medical imaging or therapy.[4,5] Most recently, functionalization of graphene,[8] a new type of nano-object, by polymer chains,[9] including PEG chains,[10–13] has drawn a lot of attention. Graphene and carbon nanotubes are closely related allotropes of carbon: graphene consists of a single sheet of sp^2 carbon atoms densely packed in a honeycomb crystal, and carbon nanotubes can be seen as rolled-up graphene sheets. The properties conferred on these carbon nano-objects by PEG layers are ultimately related to the conformation the PEG chains adopt once end-attached to their surfaces. Thus, gaining some insights into the conformational behavior of PEG chains attached to graphene-like surfaces is important for a better predictability of the properties of PEGylated carbon nano-objects. Yet, whereas the conformation and structure of PEG chains end-attached to many types of surfaces have been widely studied, transposition of these results to the case of PEG on graphene-like surfaces is not

Laboratoire d'Electrochimie Moléculaire, UMR 7591 CNRS, Univ Paris Diderot, Sorbonne Paris Cité, 15 rue Jean-Antoine de Baïf, F-75205 Paris Cedex 13, France. E-mail: anne@univ-paris-diderot.fr, demaille@univ-paris-diderot.fr

† Electronic supplementary information (ESI) available: Additional experimental details, synthesis of Fc–PEG_{3400}–pyrene, ^{1}H-NMR and MALDI-TOF characterization of Fc–PEG–OH and Fc–PEG–pyrene, scanning electron microscopy images of the combined AFM-SECM probes and tapping mode Mt/AFM-SECM amplitude and current approach curves. See DOI: 10.1039/c3cp54720e

a priori straightforward. One of the reasons for this is the exceptionally strong hydrophobic character of the latter surfaces[14] which may result in direct interactions of the surface with the PEG chain backbone itself. Indeed, even though PEG is primarily known for its hydrophilicity, it also displays some hydrophobic character which sometimes provokes unexpected polymer adsorption on certain kinds of surfaces.[15] Similarly, a recent theoretical study predicted that the structure of PEG layers end-attached to graphene-like surfaces should be greatly perturbed by the intense van der Waals forces resulting from the dense arrangement of carbon atoms in these materials.[16] Of course if the free-end of the attached PEG chain bears a molecular label, its interaction with the carbon surface may also alter the overall chain conformation, further complicating the picture. For all of these reasons, it is desirable to develop experimental approaches allowing the conformational behavior of end-attached PEG layers on graphene-like surfaces in aqueous solution to be probed.

In order to address this issue, we propose in the present work to assemble and to study the conformational and dynamical properties of a layer of PEG chains end-attached to highly oriented pyrolytic graphite (HOPG), a surface consisting of well-ordered stacked layers of graphene. Hence, we expect that our work can provide some insights into the behavior of PEG layers attached to isolated graphene sheets or carbon nanotubes, as far as the PEGcarbon surface interactions are concerned, leaving obviously aside any nano-size effect. Surprisingly, and in spite of the fact that numerous methods exist to attach molecules or macromolecules to HOPG, either covalently[17–19] or non-covalently,[20–23] we found only one experimental report describing end-attached PEG (actually PEG 4-mer)[13] layers on this surface. Yet, beyond being a model for graphene-based objects, HOPG has many other advantages that we intend to exploit in the present study. It is notably a very good electrode material[24–26] which allows the straightforward *in situ* interrogation of molecular layers formed at its surface by using robust electrochemical methods.[20–23] An extra benefit of HOPG is its nanometer-scale smoothness which makes it possible to characterize molecular layers using local probe techniques, such as atomic force microscopy (AFM).

In the present case a molecular layer of PEG_{3400} chains bearing a redox-label at one of their extremities and an anchoring pyrene foot at the other was allowed to self-assemble onto HOPG. The strong adsorption of the pyrene moiety onto graphite planes allowed the robust non-covalent end-attachment of the PEG chains to the HOPG surface. The properties of the PEG layer were studied *via* the electrochemical interrogation of the redox label decorating the free-end of the terminally attached chains. Cyclic voltammetry was used to accurately measure the surface coverage in PEG chains, which is a crucial parameter for studying end-attached layers, but also to gain insights into the microscopic environment experienced by the free end of the anchored chain. The PEG layer was also studied by molecule-touching atomic force electrochemical microscopy (Mt/AFM-SECM), an innovative local probe microscopy technique using a microelectrode for combined local force and electrochemical measurements.[27–29] This technique uniquely allowed both the overall chain conformation and the position of the redox-labeled free-end of the chains over the anchoring surface to be determined. Overall it is shown that the strongly adsorbing nature of HOPG results in a complex coverage-dependent behavior of the PEG layer but that controlled formation of ''ideal'' and potentially useful end-grafted PEG layers on HOPG is possible.

Experimental

PEG derivatives and materials

The ferrocene Fc-end labeled linear poly(ethylene glycol) PEG chain Fc–PEG–OH (PEG = $(CH_2CH_2O)n$ with $n \approx 79$, avg. M_W PEG 3400) was synthesized and obtained as an analytical sample as described previously.[27,30] The pyrene-terminated Fc–PEG product, Fc–PEG–pyrene, was prepared from Fc–PEG–OH, and was thoroughly characterized by ^{1}H NMR and MALDI-TOF mass spectroscopies as detailed in ESI.† The characterization demonstrated that the Fc–PEG–pyrene sample was absolutely free of the parent compound Fc–PEG–OH. This extreme degree of purity was essential for the interpretation of the data reported here.

1-Pyrene-methylamine hydrochloride (95%) was obtained from Aldrich. Triethylamine was a puriss. p.a. $\geq$99.5% grade product obtained from Sigma-Aldrich. Sodium perchlorate ($NaClO_4$) monohydrate was purchased from Fluka. Other commercial chemicals were of reagent grade or better quality and used as received. All aqueous solutions were made using Milli-Q purified water (Millipore). All solutions used for AFM-SECM experiments were filtered before use on a 0.22 μm nylon VWR syringe filter.

Assembly of a Fc–PEG layer on HOPG

The freshly peeled HOPG surface (Mersen, France) was mounted as the bottom of an O-ring cell and covered with $\sim$200 μL of an aqueous solution containing the Fc–PEG derivative (either Fc–PEG–pyrene or Fc–PEG–OH), at a concentration chosen in the 5–200 μM range. After 30 min, the Fc–PEG modified HOPG surface was thoroughly washed with MQ water. For subsequent characterization of the Fc–PEG layer, by cyclic voltammetry or Mt/AFM-SECM, the cell was filled with $\sim$600 μL of an aqueous 1 M $NaClO_4$ electrolyte. If AFM imaging in air was then intended, the surface was rinsed anew with water and dried under a flux of nitrogen.

Cyclic voltammetry (CV)

Cyclic voltammetry characterization of the HOPG surfaces modified by the Fc–PEG derivatives was either carried out using the ''substrate'' channel of the home-made AFM-SECM bipotentiostat (see below), or a dedicated custom designed voltammetry set-up.[30] All potentials in this work are reported *versus* SCE (KCl saturated calomel reference electrode). The temperature in electrochemical experiments was 20 °C.

Fabrication of the combined AFM-SECM probes

The probes were hand-fabricated from bent, flattened and etched 60 μm-diameter gold wires according to a procedure adapted from the literature,[31] and largely detailed elsewhere.[32] The flattened part of the wire acted as a flexible cantilever (spring constant ~0.5–3 N m^{-1}, fundamental flexural frequency ~2–3 kHz), bearing a conical tip formed by etching. By adjusting the etching conditions tips with a spherical apex of ~100 nm or down to ~20 nm in radius could be selectively produced. The actual tip radius was measured from MEB images (see Fig. S6 in ESI†). The tip was fully insulated by deposition of an electrophoretic paint, and glued onto an AFM chip. The apex was selectively exposed in order to act as a current-sensing nanoelectrode.

AFM and combined AFM-SECM experiments

AFM images in air and in water were obtained using a Molecular Imaging PICOSPM I AFM microscope (Agilent) operating in tapping mode and using commercial Multi-75G probes (Budget Sensor). The Mt/AFM-SECM experiments were carried out using the same PICOSPM I instrument modified to be operated in SECM mode[32] and using hand-fabricated AFM-SECM probes. A platinum wire was then used as a counter-electrode, and the reference electrode was a Pt wire coated with an electropolymerized polypyrrole film, as previously described.[29] A homemade bipotentiostat was used to control the potential applied to the substrate and to the probe independently. Cyclic voltammograms could be recorded at the substrate while maintaining a constant bias at the probe. For the probe and substrate current acquisitions, high (10 pA V^{-1}) and low (20 μA V^{-1}) gain current measuring circuits were used. The probe-current signal was passed through a 10 Hz low-pass analogue filter. The substrate potential was generated by a PAR 175 programmer. The probe-current data were corrected from the nonspecific leakage current resulting from the imperfect insulation of the connecting wires. This current is nonspecific and independent of the tip-to-substrate distance and of the probe and substrate potential.

Results and discussion

Fc–PEG–pyrene as a model functional molecule designed to form self-assembled redox monolayers onto HOPG

In the present work the Fc–PEG–pyrene molecule depicted in Scheme 1 was home-synthesized as detailed in the ESI,† with the purpose of forming self-assembled layers onto HOPG surfaces.

This linear molecule consists of a flexible, water soluble PEG_{3400} chain, ~79 monomers long, bearing at one of its extremities a redox moiety, ferrocene (Fc) known for its uncomplicated electrochemistry, while its other extremity bears a pyrene ring. The pyrene moiety is capable of robustly adsorbing onto graphite planes,[33] and is thus expected to be an effective anchoring foot for the end-attachment of the Fc–PEG chain onto HOPG, as was observed for pyrene-modified small molecules,[20–23] or linear macromolecules so-attached to graphene-like surfaces, such as DNA onto HOPG,[22] PEG onto carbon nanotubes[6,7] and graphene.[13] The PEG chain itself obviously attracts interest due to its wide use as a biocompatible polymer which, once end-attached to a surface, efficiently prevents non-specific protein adsorption. The Fc–PEG–pyrene molecule also constitutes a good model of a functional molecule that one would want to spontaneously end-attach onto graphene planes in such a way that its functional free extremity (here the Fc head) is presented to the solution in a controlled way, and positioned at some predefined distance from the surface.[34] In the present case, the Fc-head being borne by a flexible polymer chain, its position above the surface is not expected to be fixed, but rather to be statistically defined, and to be in the order of the Flory radius of the chain, R_F ~ 5 nm.[30]

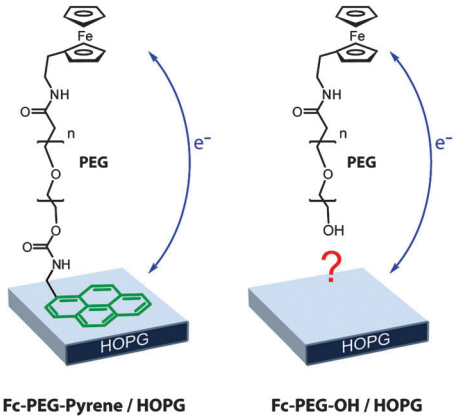

Scheme 1 Molecular structures of the Fc–PEG conjugates considered in this work. The molecules are shown in interaction with a HOPG electrode surface. (left) Fc–PEG_{3400}–pyrene molecule (n ~ 79), designed to end-adsorb onto HOPG *via* its pyrene foot. (right) Parent Fc–PEG_{3400}–OH molecule lacking the anchoring pyrene foot and possibly adsorbing onto HOPG in an unpredicted way.

Generally speaking, formation of well-defined end-grafted layers of water-soluble molecules comprising a pyrene foot, a linker, and a functional free end, onto HOPG requires that (i) the interaction between the pyrene anchoring group and the graphite planes is strong enough to compensate for the solubility of the molecule. (ii) Other parts of the molecule, such as the linker or the functional group, themselves are not prone to interact (adsorb) with the HOPG surface. In the present case these general problems are particularly acute since: (i) the PEG chain endows the Fc–PEG–pyrene molecule with a high water solubility. (ii) Yet molecular dynamics simulations of PEG layers end-grafted onto HOPG (or graphene) surfaces have predicted that the chain backbone, in spite of its hydrophilicity, should paradoxically be prone to adsorption onto these surfaces.[16] Moreover, the hydrophobic nature of the cyclopentadienyl rings of ferrocene may favor adsorption of the Fc-heads from aqueous media. Indeed adsorption of ferrocene derivatives onto HOPG has been reported in the literature,[35] and also observed by us for the simple ferrocenemethanol.

For all of these reasons we systematically compared here the adsorption behavior of Fc–PEG–pyrene to that of the parent compound Fc–PEG–OH (Scheme 1, right), which lacks the anchoring pyrene foot.

Forming a self-assembled layer of Fc–PEG–pyrene chains on HOPG. Characterization by cyclic voltammetry

Assembly of the Fc–PEG–pyrene layer onto freshly cleaved HOPG electrode surfaces was carried out by covering the surface, secured in an O-ring cell, with ~200 μL of a 5–200 μM Fc–PEG–pyrene solution in MQ water. The Fc–PEG–pyrene solution was left in contact with the surface for 30 minutes. The surface was then thoroughly rinsed with MQ water, and the cell filled with a 1 M $NaClO_4$ aqueous electrolyte. Cyclic voltammograms (CV's) were then recorded at the modified HOPG surface, by scanning its potential between 0.0 V/SCE and +0.4 V/SCE, at scan rates ranging from 0.1 V s^{-1} to 20 V s^{-1} and recording the resulting current. One can see from Fig. 1A, that a well-defined peak-shaped current signal is then obtained (blue trace), which contrasts with the featureless capacitive signal recorded at a bare HOPG surface (dashed trace).

The peak current of the signal recorded at the Fc–PEG–pyrene modified surface was observed to increase linearly with the scan rate and the peak-to-peak separation was small, in the order of 10 mV at 20 V s^{-1}. These characteristics are typical of an electrode-attached redox species undergoing fast (Nernstian) electron transfer. The voltammograms therefore correspond to the one-electron reversible oxidation–reduction of the Fc/Fc^+ heads of the surface confined Fc–PEG chains.

The apparent standard potential ($E^{\circ\prime}$) of the Fc heads, given by the half-sum of the anodic and cathodic peak potentials, was systematically found to fall in the 0.21–0.15 V/SCE region (see below), *i.e.* in a potential region encompassing the standard potential of ferrocenedimethanol (E° = 0.21 V/SCE)[36] and of the Fc-head of Fc–PEG chains free in solution (E° = 0.15 V/SCE, as we measured it previously).[27] All of the above clearly indicates that, as expected, Fc–PEG–pyrene assembled spontaneously onto the HOPG surface.

The stability of the layer was assessed by monitoring the persistence of the CV signal with time, the surface being kept in the $NaClO_4$ electrolyte solution either at open-circuit or biased at +0.0 V/SCE. It was found that the signal remained unchanged for many hours. However the layer was found to be less stable when the electrode was held at a potential more positive than ~+0.4 V/SCE. Understandably immersion of the modified HOPG surface in organic solvents, such as acetonitrile, resulted in an immediate and complete signal loss, *i.e.* in the desorption of the Fc–PEG–pyrene layer.

The surface coverage in Fc–PEG-chains of the modified HOPG electrodes was determined by integration of the peak-shaped CV signals, which yielded Q, the total charge passed to oxidize/reduce the Fc-heads present on the surface. Dividing this charge by the "real" surface area of the HOPG electrode, and by the Faraday constant, yielded Γ_{Fc}, the surface coverage in Fc heads. Due to its extreme smoothness the "real" surface area of the HOPG electrode can be legitimately considered as its geometric surface area, as a result very accurate and reliable Γ_{Fc} values could be derived. Since there is one Fc head of the PEG chain the surface coverage in chains, Γ, is simply $\Gamma = \Gamma_{Fc}$. Surface coverages in the 5–25 pmol cm^{-2} range were obtained, depending on the concentration of the Fc–PEG–pyrene solution used for adsorption, $C_{sol.}$. More precisely, and as seen from the adsorption isotherm reproduced in Fig. 2A, Γ was observed to increase almost linearly with $C_{sol.}$ up to ~50 μM. For higher concentrations (50 μM < $C_{sol.}$ ≤ 200 μM) the Γ *vs.* $C_{sol.}$ variation described a slightly descending plateau, with a maximum (saturating) coverage value around Γ ~ 25 pmol cm^{-2}.

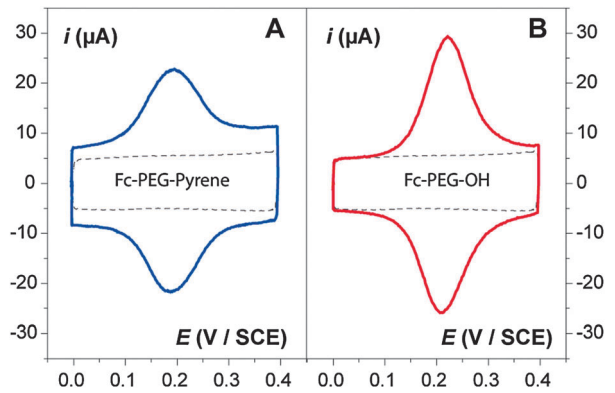

Fig. 1 Cyclic voltammograms recorded at HOPG surfaces bearing (A) a Fc–PEG–pyrene layer, and (B) a Fc–PEG–OH layer. The dashed trace is the typical purely capacitive signal recorded at a freshly cleaved bare HOPG surface. Surface coverages: (A) 10.5 pmol cm^{-2}. (B) 18.4 pmol cm^{-2}. Adsorption was carried out on a 20 μM Fc–PEG derivative in water. Aqueous 1 M $NaClO_4$ electrolyte. Scan rate 1 V s^{-1}. T = 20 °C.

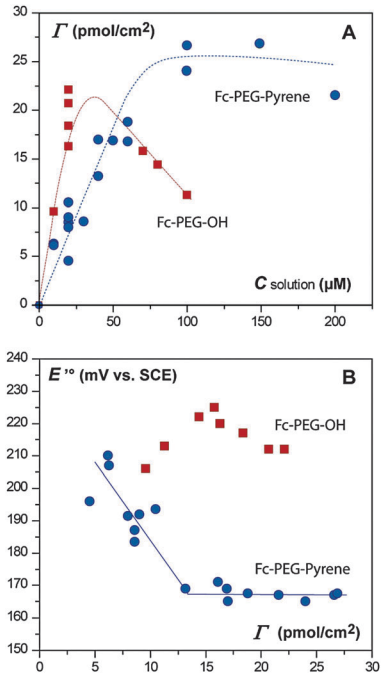

Fig. 2 Characteristics of the Fc–PEG–pyrene (blue dot symbols) and of the Fc–PEG–OH (red square symbols) layers formed on HOPG as determined by cyclic voltammetry (CV). (A) Adsorption isotherm: surface coverage in chains as a function of the concentration in Fc–PEG derivatives of the solution used for adsorption ($C_{sol.}$ in text). (B) Apparent standard potential ($E^{\circ\prime}$) of the Fc head as a function of the chain coverage. The lines are guide to the eye. Aqueous 1 M $NaClO_4$ electrolyte. T = 20 °C.

Importantly we verified that, for any given value of $C_{sol.}$, Γ did not increase further if the adsorption time was increased beyond $\sim$30 min, *i.e.* the Γ values discussed here correspond to equilibrium coverages. It is also interesting to note that even the highest Γ values measured here are much lower than the coverage value corresponding to a close-packed layer of adsorbed pyrene rings, which, taking 1 nm^2 for the foot-print of pyrene, would be in the order of $\sim$166 pmol cm^{-2}. Hence saturation of the HOPG surface is controlled by the foot print of the chain on the surface. Therefore, determining the value of Γ can yield the first insights into the conformation of the Fc–PEG–pyrene molecule on the surface. Indeed like for any linear polymer, the conformation of Fc–PEG–pyrene once end-grafted is expected to be dictated by the average distance separating neighboring chains on the surface, denoted s and related to Γ by $s = 1/\sqrt{N\Gamma}$. Two extreme regimes can be reached depending on the value of s with respect to R_F: if $s \gg R_F$ the chain adopts a coil-like (so-called mushroom) conformation, its monomers explore a hemi-spherical volume of radius $\sim R_F$ extending away from the anchoring point, and there is no interaction between neighboring chains. If at the opposite $s \ll R_F$ then the chain extends toward the solution to avoid such interactions, forming a so-called polymer brush of height $h > R_F$.[37,38] Practically the brush regime has been predicted to be reached for $s \leq R_F/4$.[39]

In the present case the range of Γ explored (5–25 pmol cm^{-2}) corresponds to s values going from 2.5 nm to 5.8 nm, *i.e.* comprised in the range extending slightly beyond and above R_F. Hence, the chains on the surface studied here are expected to adopt a non- to a weakly-overlapping mushroom conformation.[39]

Finally, in that context, attainment of a saturating coverage in Fc–PEG–pyrene at the plateau of the adsorption isotherm can be explained based on the peculiar behavior of end-anchored chains: saturation is reached when the energy penalty associated with the insertion of a new chain in the layer, which would require further stretching of the anchored chains, no longer compensates the energy gained by forming a new pyrene–HOPG bond.

Of course the above discussion is only valid provided the Fc–PEG–pyrene chains are effectively end-attached, *i.e.* if the pyrene foot does play its role of an anchor and no other part of the molecule interacts with the HOPG surface. In order to verify if such is the case we carried out the exact same adsorption and characterization steps as above but replacing Fc–PEG–pyrene by Fc–PEG–OH. Much to our surprise we observed that voltammograms recorded at HOPG surfaces modified by either of the Fc–PEG-derivatives are, at first glance, similar (compare Fig. 1A with Fig. 1B). Hence, not only Fc–PEG–OH and Fc–PEG–pyrene molecules both adsorb onto HOPG, but they also form layers of comparable chain coverage. However a closer examination of the cyclic voltammetry results shows that there are meaningful differences in the adsorption behavior of Fc–PEG–pyrene and Fc–PEG–OH. Firstly, the stability of the Fc–PEG–OH layer upon repeated potential scanning was found to be somewhat less than that of the Fc–PEG–pyrene layer. Secondly the quantitative characteristics of the voltammograms recorded at HOPG electrodes modified by either of the two Fc–PEG derivatives are not exactly the same. The peaks of the CV recorded at the Fc–PEG–pyrene modified surface tend to be broader than those recorded at Fc–PEG–OH bearing surfaces: in the latter case the width at half-peak height was 90–105 mV, whereas in the former case it ranged from 98 mV up to 130 mV depending on the concentration of the adsorption solution. But most importantly the adsorption isotherms of the two Fc–PEG derivatives differ markedly (see Fig. 2A). Rather than being plateau-shaped, as observed for Fc–PEG–pyrene, the Γ *vs.* $C_{sol.}$ variation for Fc–PEG–OH is clearly peak-shaped: Γ initially rapidly increases with $C_{sol.}$, faster than what was observed for Fc–PEG–pyrene, but then sharply decreases when $C_{sol.}$ is increased beyond $C_{sol.} \sim 75$ μM. These differing adsorption isotherms are an indication that the interactions of each of the two Fc–PEG derivatives with HOPG are thermodynamically distinct, suggesting that differing parts of the molecules adsorb on the surface. This is an indication that adsorption of the pyrene foot at least partly drives the formation of the Fc–PEG–pyrene layer.

Another major difference between the CV behavior of the two Fc–PEG derivatives is that, as illustrated in Fig. 2B, the apparent standard potential ($E^{\circ\prime}$) of the Fc head displays a clear dependence on Γ for Fc–PEG–pyrene whereas it is roughly constant for Fc–PEG–OH. More precisely, at low coverage ($\sim$5 pmol cm^{-2}) the Fc–PEG-derivatives display a similar standard potential around +210 mV/SCE. However, upon increasing Γ up to $\sim$12.5 pmol cm^{-2} the $E^{\circ\prime}$ value for Fc–PEG–pyrene decreases almost linearly down to $\sim$+165 mV/SCE, and then remains constant for higher coverages (see Fig. 2B).

The fact that the $E^{\circ\prime}$ value measured both for the Fc–PEG–OH layers and for the low coverage Fc–PEG–pyrene layers is significantly higher than the standard potential of freely diffusing Fc–PEG chains ($\sim$+150 mV/SCE) indicates that in these layers the Fc^+ form is destabilized. This in turn suggests that the Fc-heads then experience a hydrophobic environment. In contrast the fact that the $E^{\circ\prime}$ value found for high coverage Fc–PEG–pyrene layers is relatively close to the standard potential of free Fc–PEG chains indicates that within ''dense'' Fc–PEG–pyrene layers the Fc-heads mostly experience an aqueous environment. Hence, the variation of $E^{\circ\prime}$ with Γ observed for intermediate Γ values can be interpreted as a change in the environment of the Fc heads, which from hydrophobic becomes more solution-like as Γ is gradually increased.[40] This change is complete when Γ exceeds a critical value of $\sim$12.5 pmol cm^{-2}. It is tempting to ascribe this variation to a gradual change of the Fc–PEG chain conformation of Fc–PEG–pyrene with Γ resulting in a change in the position of the Fc head within the layer. However cyclic voltammetry cannot yield information regarding the key issues of the PEG chain conformation.

Therefore the Fc–PEG–pyrene bearing surface was characterized by Mt (Molecule touching)/AFM-SECM, an original combined local probe technique we introduced earlier[27,28] which offers the unique possibility of *directly* probing the overall conformation of redox end-labeled nanometer sized chains, such as Fc–PEG,[27] or Fc–DNA,[41] terminally attached to electrode

surfaces, while simultaneously electrochemically sensing their redox head.

Characterizing the Fc–PEG–pyrene layer on HOPG by contact mode Mt/AFM-SECM: analyzing force and current approach curves

In a typical experiment a combined home-fabricated gold AFM-SECM probe, acting both as a microelectrode and a force sensor, was approached *in situ* (aqueous 1 M $NaClO_4$) from Fc–PEG–pyrene modified HOPG surfaces. For a better force sensitivity a probe characterized by a rather large tip radius ($R_{tip} \sim 100$ nm) was selected. The probe and the substrate were biased at potentials sufficiently remote from $E^{\circ\prime}$ for the Fc heads to be, respectively, oxidized and reduced at diffusion controlled rates (*i.e.* infinitely fast):[27] E_{tip} = +0.3 V/SCE and E_{sub} = 0.0 V/SCE. The tip deflection and tip current (i_{tip}) were simultaneously recorded during the approach. The tip deflection scale was converted into an actual force scale by making use of the spring constants of individual tips derived by the thermal noise method.[42] The actual tip–substrate distance, d, was derived from the tip deflection, as classically done in AFM.[42] Finally, force (F) *vs.* d and i_{tip} *vs.* d approach curves such as those presented in Fig. 3A and B were obtained. Each of these two figures present data acquired over HOPG substrates bearing either a relatively low coverage Fc–PEG–pyrene layer ($\Gamma \sim 8.7$ pmol cm^{-2}, curve I) or a high coverage layer ($\Gamma \sim 23.9$ pmol cm^{-2}, curve II). For comparison data acquired over a bare HOPG substrate are also reproduced in purple trace.

Force approach curves. By examining the force approach curves I and II shown in Fig. 3A one can see that upon approaching the tip from a Fc–PEG–pyrene modified surface the originally flat deflection trace bends upward, indicating that purely repulsive forces are sensed. Importantly this repulsive part of the approach curve is not observed when an AFM-SECM tip is approached from a *bare* HOPG surface (see Fig. 3A, purple trace), a jump-to-contact descending peak, due to attractive van der Waals forces, is then observed instead. Hence the repulsive part of the force approach curves in Fig. 3A corresponds to the tip starting to compress the Fc–PEG chains. Such smoothly rising force curves are typical of AFM approach curves recorded upon compressing end-attached polymer layers,[43,44] including PEG layers.[45] The first interesting observation is made by comparing curves I and II: it is seen that, upon approaching the tip from the surface, the onset of force is detected "later" (*i.e.* for smaller d values) for the lower coverage layer (curve I) than for the high coverage layer (curve II). This is the first, qualitative evidence that the high coverage layer is overall "thicker" than the low coverage layer.

More detailed information regarding the structure of the Fc–PEG–pyrene chain in these layers can be gained by quantitative force curve analysis as follows.

Compression of end anchored chains by a spherical tip of a large radius R_{tip} (*i.e.* $R_{tip} \gg R_F$) has been theoretically predicted to give rise to a force law of the form: $F = F_0 \exp(-d/d_0)$, where F_0 is a characteristic force, related to the chain coverage Γ, and where d_0 is a distance characterizing the layer thickness.[46]

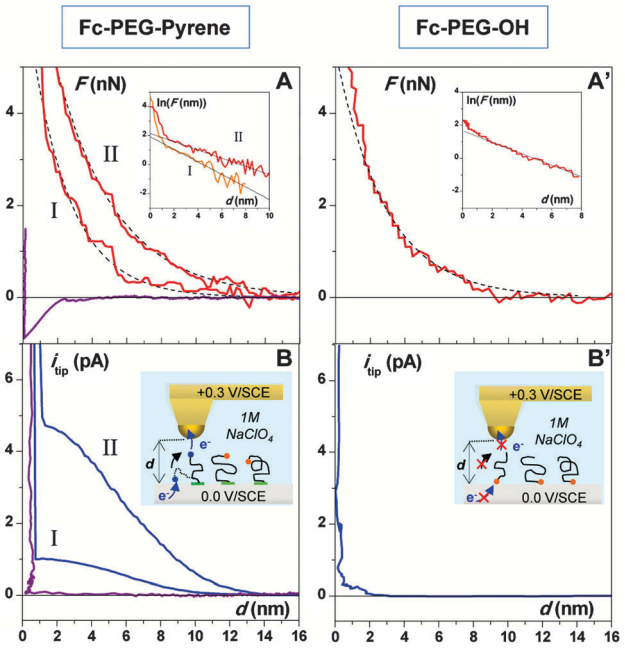

Fig. 3 Contact mode Mt/AFM-SECM approach curves recorded *in situ* over a HOPG substrate either bare (left panel purple traces), bearing Fc–PEG–pyrene layers at two different coverages (left panel, curves I and II), or bearing a Fc–PEG–OH layer (right panel). The force applied by the tip to the layer (F) is plotted in A and A′. The simultaneously acquired tip current signal (i_{tip}) is plotted in B and B′. The abscissa (d) is the actual tip–substrate distance (see insets in B and B′). The chain coverage in Fc–PEG–pyrene was 8.7 pmol cm^{-2} and 23.9 pmol cm^{-2} for curves I and II, respectively. The chain coverage in Fc–PEG–OH was 12 pmol cm^{-2}. The dotted curves in A and A′ are fitting curves (see text). The insets in A and A′ are ln(F) *vs.* d plots. For the acquisition of the approach curves, the tip and substrate potentials were set to E_{tip} = +0.30 V/SCE, E_{sub} = 0.0 V/SCE. Approach rate 10 nm s^{-1}. Aqueous 1 M $NaClO_4$ electrolyte. T = 20 °C. Curves I and II in A and B were acquired with the same probe.

The exact expressions of F_0 and d_0 depend on the chain coverage regime. At low coverage, in the mushroom regime, $F_0 = 72\pi k_B T R_{tip} \Gamma N$, and the value expected for d_0 is R_g, the radius of gyration of the chain given by $R_g = R_F/\sqrt{6}$.[47] At high coverage, in the brush regime, $F_0 = 100 k_B T R_{tip} h (\Gamma N)^{3/2}$, where h is the brush height, and $d_0 = h/(2\pi)$.[48] Hence, in the present case exponential variations of F with d were sought for. They were clearly observed for both of the Fc–PEG–pyrene layers examined, as can be seen from the ln(F) *vs.* d plots shown in Fig. 3A (inset). From such plots experimental values of $F_0 = 6.9 \pm 1.2$ nN, $d_0 = 2.3 \pm 0.2$ nm and $F_0 = 8.7 \pm 1.0$ nN, $d_0 = 3.5 \pm 0.3$ nm were respectively obtained for the low and high coverage layers. These parameters allowed the entire experimental force curves to be nicely reproduced by exponential force laws at least down to $d \sim 1$ nm (dashed traces in Fig. 3A).

For the lowest coverage layer, we note that the value derived for d_0 is close to the value of $R_g \sim 2$ nm typical of PEG_{3400} chains. Moreover in this case the expression of F_0 corresponding to the mushroom case yields a value of Γ of (12 ± 2) pmol cm^{-2}, which is reasonably close to the actual coverage value of 8.7 pmol cm^{-2} obtained by CV for this surface. In contrast, the brush scenario was found to be much

less consistent since it yielded a value of h = 15 ± 2 nm ($\gg R_F$), indicative of some degree of chain extension, incompatible with the low coverage value of this particular Fc–PEG–pyrene layer.

Hence one can conclude from the analysis of the force curves that, for the low coverage layer, the Fc–PEG–pyrene chains are effectively end-attached to the HOPG surfaces and do form an array of adjacent hemispherical mushrooms.

Considering now the high coverage layer (Fig. 3A, curve II), we note that the d_0 value obtained (~3.5 nm) is significantly higher than the one derived for the low coverage layer (Fig. 3A, curve I), confirming quantitatively that the chains are more extended toward the solution at high coverage. However both the mushroom and the brush model fail to correctly describe such a layer: d_0 is markedly larger than R_g while the brush model yields a large h value of ~22 nm and an abnormally low Γ value of ~7.5 pmol cm^{-2}. These experimental results fall in line with the theoretical behavior expected for ''ideal'' end-grafted chains grafted at ''intermediate'' coverage where the inter-chain distance, s = 2.6 nm here, is sufficiently small as compared to R_F for the chains to elongate toward the solution, but not enough for the brush regime to be met. We thus demonstrated that the Fc–PEG–pyrene chains are indeed in the so-called overlapping mushroom regime within the high coverage layer studied here.

Hence analysis of the force approach curves demonstrated that *both* at low and high coverages the Fc–PEG–pyrene chains form ''ideal'' end-attached layers on HOPG. Yet there remains a question, to which force measurements alone cannot bring an answer: where are the Fc-heads located within the Fc–PEG–pyrene layers? Because in Mt/AFM-SECM the combined tip also acts as a microelectrode, which specifically addresses the Fc heads, the answer to this question can be found by considering the current approach curves I and II presented in Fig. 3B.

Current approach curves. One can see in Fig. 3B that upon approaching the tip toward the surface a current starts flowing through the tip from d ~ 12 nm for curve I and d ~14 nm for curve II, which nicely corresponds to the onset of force as observed from Fig. 3A. Upon pushing the tip further toward the substrate the current increases in intensity until a plateau is reached in the d ~ 3 nm region. For d < 0.5 nm an intense tunneling/short circuit current is recorded. Importantly, we observed that, provided it was brief enough, this high current regime did not result in disrupting the PEG layer. This was demonstrated by the fact that the current retraction curve recorded upon withdrawing the tip from the surface was similar to the current approach curve. Such a result also shows that the chains were not displaced by the incoming tip. As expected, for a bare HOPG surface the current approach curve solely displays the tunneling/short circuit region (purple trace in Fig. 3B). Hence, as previously demonstrated for layers of Fc-labeled flexible chains such as PEG or DNA end-attached to gold, the plateau-shaped current approach curve recorded here at the Fc–PEG–pyrene modified HOPG surfaces is due to the tip electrochemically interrogating the Fc heads.[27,28] Upon contacting the tip the Fc heads are oxidized to their Fc^+ form which diffuses to the substrate where they are re-reduced, as schematized in Fig. 3B (inset). Such a redox cycling, classically referred to as SECM positive feedback,[49,50] or elastic bounded diffusion positive feedback here,[27] generates an easily measured stationary tip current whose intensity depends both on the number of Fc heads addressed by the tip and on the rate at which electrons are shuttled from the substrate to the tip by the Brownian motion of the chain. The current initially increases with decreasing d, since the tip–substrate travel distance is made smaller, and then plateaus as a result of over-confinement of the chains under the tip, which slows down chain dynamics.[28]

The fact that typical elastic bounded diffusion current approach curves were recorded here demonstrates that at least some of the Fc heads of the Fc–PEG–pyrene chains are free to explore a volume expanding up to some ~12–14 nm away from the surface, just as expected for chains end-grafted *via* their pyrene foot. Yet, interestingly, we note that the intensity of the current approach curves I and II is in a ratio of ~1 : 5 whereas the corresponding chain coverages, which should set the number of chains addressed by the tip, are only in a ratio of 1 : 2.7. A possible interpretation for this result is that the tip current recorded for the low coverage layer is abnormally low. This would indicate that in such a layer either the motional dynamics of the Fc heads is slowed, or more likely that some ~50% of the Fc heads are then inaccessible to the tip. Permanent adsorption of some of the Fc heads on the HOPG surface could explain this behavior, as this would of course make these Fc heads impossible to address by the tip until it virtually contacts the substrate surface (*i.e.* d < ~1 nm). Such an interpretation is compatible with the above-detailed analysis of the voltammetric signal of Fc–PEG–pyrene layers which indicated that, *only in low coverage layers*, the Fc heads experienced a hydrophobic environment, which probably is the HOPG surface itself. Yet at this stage it is not clear how adsorption of the Fc-heads could be compatible with the ideal mushroom conformation displayed by the chains in these layers.

Insights into this question can be gained by considering the contact mode-Mt/AFM-SECM F *vs.* d and i_{tip} *vs.* d approach curves recorded at a HOPG surface bearing a Fc–PEG–OH layer, and presented in Fig. 3A′ and B′. One can see that the force curve is reasonably well described by an exponentially F *vs.* d variation (dotted line) characterized by F_0 ~ (7.0 ± 0.6) nN, and d_0 = (2.1 ± 0.5) nm. These values are found to be compatible with the mushroom scenario since they yield R_g = 2.1 nm and Γ = 12 pmol cm^{-2}, which agrees well with both the chain dimension and the CV-derived chain coverage. These results show that the Fc–PEG–OH chains are end-attached to the surface, and form an array of polymer mushrooms, just like the Fc–PEG–pyrene chains. However, comparison of the current approach curves recorded for these two Fc–PEG-derivates (Fig. 3B and B′) reveals a striking difference between the layers: whereas an intense tip current approach curve was recorded for the Fc–PEG–pyrene layer in the 2 nm < d < 12 nm region absolutely no current is observed for the Fc–PEG–OH layer in the same region. The absence of tip current shows that, albeit

the probe clearly compresses the Fc–PEG–OH layer, as judged from the force curve in Fig. 3A′, the Fc heads remain totally inaccessible to the tip at least down to $d \sim 2$ nm, where the onset of tunneling then blurs the picture. These seemingly conflicting force and current data actually lead to the conclusion that, as shown in Fig. 3B′ (inset), the Fc head actually plays the role of the anchoring group of the Fc–PEG–OH chain. As a result the chain is indeed end-attached to the surface, *via* Fc–HOPG interactions, but the Fc head being adsorbed onto the surface is not sensed by the tip. Such a picture is also fully consistent with the CV results which indicated that the environment "seen" by the Fc heads of the Fc–PEG–OH chains was different from the "aqueous" medium experienced by the Fc-heads in "high"-coverage Fc–PEG–pyrene layers. Having now shown that the Fc head can play the role of an anchor for PEG chains on HOPG finally allows us to understand the seemingly paradoxical behavior of PEG chains in the low coverage Fc–PEG–pyrene layer as evidenced above by analysis of the Mt/AFM-SECM data: within this layer half of the chains were attached *via* their pyrene foot and half *via* their Fc heads, all were thus effectively behaving as end-attached chains but only those attached *via* their pyrene foot gave rise to a tip current.

Overall the above Mt/AFM-SECM analysis showed that whereas Fc head-HOPG interactions are sufficiently strong to induce "Fc head-on" adsorption of Fc–PEG derivatives, Fc–PEG–pyrene does display the expected tendency of rather attaching to the HOPG surface *via* its pyrene foot. Some degree of "Fc-head-on" attachment of Fc–PEG–pyrene is nevertheless present in low coverage layers, but much less (if any) in high coverage layers. Most interestingly transition between these low and high coverage regimes occurs in the Γ = 12.5 pmol cm^{-2} region (as judged from Fig. 2B) which corresponds to a dimensionless surface coverage $\sigma^{\star} = \pi R_g^2/s^2$, as defined in ref. 39, of $\sim$1, indicative of the onset of mushroom overlap, *i.e.* of interchain interactions. Moreover the fact that, regardless of the anchoring extremity, we observed that the Fc–PEG-derivatives do form "ideal" end-grafted layers shows that, unlike what could have been feared from theoretical studies,[15] adsorption of the PEG chain itself onto the HOPG surface, which would have resulted in collapsed layers, did not occur significantly here.

Imaging the Fc–PEG–pyrene layer on HOPG by tapping mode AFM

Now knowing the structure of the layer formed by the Fc–PEG–pyrene on the HOPG surface the question arises concerning the uniformity of this layer over the surface of the HOPG material. To experimentally address this question we first resorted to AFM imaging carried out in tapping mode. This microscopy technique is commonly employed to study thin films on solid surfaces and provides sufficient lateral resolution to resolve nanometer-sized features. Hence Fc–PEG–pyrene layers of various surface coverages were formed onto HOPG surfaces, subsequently characterized by cyclic voltammetry in 1 M $NaClO_4$ electrolyte in order to determine the exact chain coverage, and imaged in the same medium using regular tapping mode AFM.

However, as seen in Fig. 4A, the AFM topographic image of a Fc–PEG–pyrene layer in water only revealed the typical topography of the underlying HOPG surface: a series of atomically flat plateaus separated by steps of a few nanometers in height. Such an apparently surprising result illustrates the fact that flexible end-attached chains cannot be readily imaged by AFM in a good solvent, since the chains tend to escape compression by "small" tips, *i.e.* tips having a radius comparable to the chain size ($\sim R_F$).[43,51] Both of these conditions are met here since water is a good solvent for PEG chains and the standard commercial AFM tip used to acquire the image presented in Fig. 4A has a tip radius smaller than $\sim$10 nm. Even though this

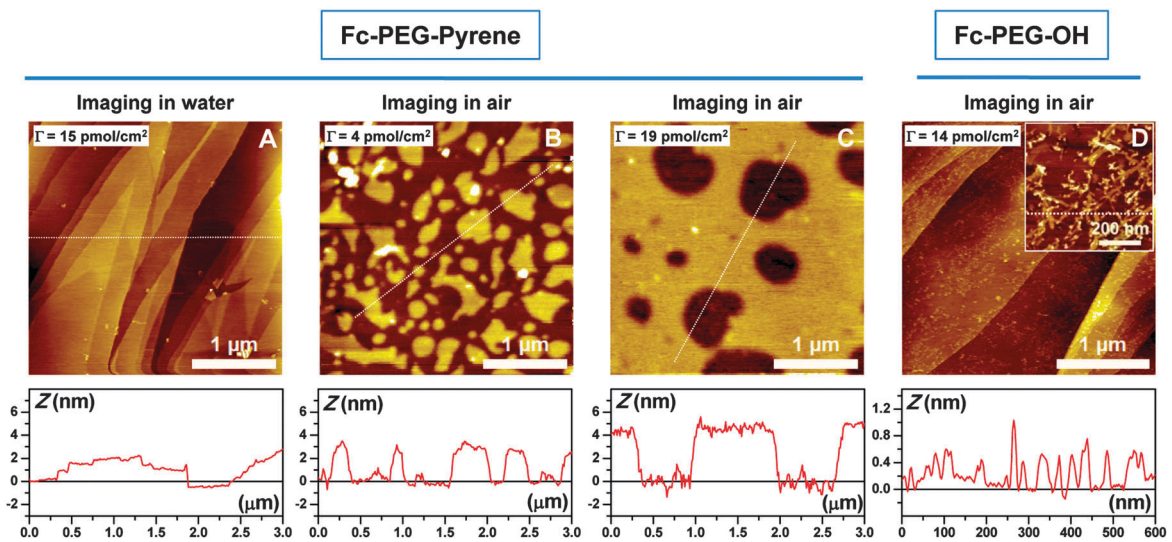

Fig. 4 Topographic tapping mode AFM images of a HOPG substrate: bearing a Fc–PEG–pyrene layer (A–C), or bearing a Fc–PEG–OH layer (D). Image (A) was acquired *in situ* (1 M $NaClO_4$ aqueous electrolyte). Images (B–D) were acquired in air. The plots below the images are cross-sections along the white dotted line shown. Commercial Mutli75G FM-probe excited at its fundamental frequency ($\sim$75 kHz in air and $\sim$30 kHz in aqueous).

result shows that regular tapping mode AFM cannot be used to probe *in situ* the distribution of the chains onto the surface, the topographic image presented in Fig. 4A shows that, as a benefit of the noncovalent binding strategy adopted here, the native structure of the anchoring HOPG surface is fully preserved. We therefore chose to also image the surface *in air* since in this case PEG chains are known to adopt stiff, hence imageable, conformations.[52] The resulting tapping mode topographic AFM images of Fc–PEG–pyrene layers displaying a low (4 pmol cm^{-2}) and a high (19 pmol cm^{-2}) chain coverage are, respectively, presented in Fig. 4B and C. We see in Fig. 4B, that, for a low chain coverage, the Fc–PEG chains appear as forming relatively large flat-top islands, up to $\sim$1 μm in width, and characterized by a very uniform height of $\sim$3 nm. Those islands are separated from one another by flat areas which seem to be devoid of PEG chains. At high surface coverage, and as seen from Fig. 4C, the Fc–PEG layer appears more as a very smooth film presenting large flat-bottom holes. Only very few objects, $\sim$1 nm in height, can be seen at the bottom of these holes. Objects of a similar height can also be seen on the film surface. Cross-sections of the topography image, across holes containing areas of the film, allow a film thickness of $\sim$4 nm to be measured.

Finally still for the sake of comparison, we also imaged in tapping mode AFM in air a layer of Fc–PEG–OH adsorbed onto HOPG; the corresponding topographic image is presented in Fig. 4D. Even though this surface displayed a chain coverage of 14 pmol cm^{-2}, comparable to the coverage in Fc–PEG–pyrene of the surface shown in Fig. 4C, the topography of these two surfaces is entirely different (compare Fig. 4C and D). Rather than forming a continuous film, the Fc–PEG–OH chains appear as an ensemble of strings 0.5–1 nm in height extending over the HOPG terraces (see inset in Fig. 4D). The correspondence between this height and the size of a PEG monomer (a = 0.35 nm) suggests that what is actually seen are bundles of flat lying PEG chains. Hence upon drying the Fc–PEG–OH films the chains simply collapse onto the HOPG surface. Such a result obviously indicates that the lack of a pyrene anchor prevents the Fc–PEG–OH chains from forming the well-defined hydrated films or islands observed for Fc–PEG–pyrene chains. Moreover, we observed that similarly nano-structured layers also formed upon adsorbing methoxy-capped PEG–pyrene chains onto HOPG (data not shown). All these results point not only to the crucial role of the pyrene foot in the formation of well-defined hydrated PEG films and nanostructures in air but also show that the ferrocene moiety played no role in this respect.

The remaining question, that regular AFM failed to answer, is: what is the actual *in situ* (*i.e. in aqueous*) distribution of the Fc–PEG chains on the HOPG surface?

Mapping the *in situ* 2D-distribution of Fc–PEG–pyrene chains on HOPG by tapping mode Mt/AFM-SECM imaging

We previously demonstrated that Mt/AFM-SECM, used in imaging mode, is a tool of choice for mapping *in situ* the 2D-distribution of redox labeled macromolecules, such as Fc–PEG chains, attached to an electrode surface. To this aim Mt/AFM-SECM simply needs to be operated in tapping mode: the AFM-SECM probe is driven into oscillation and surface-induced damping of this oscillation is used to keep the tip at a constant distance above the substrate. This distance is chosen experimentally so as to be sufficiently small for the tip to remain in electrochemical contact with the redox head of the macromolecules.

In the present case a particularly sharp ($R_{tip} \sim 20$ nm) home-made AFM-SECM probe, acoustically driven so as to oscillate at its fundamental flexural frequency, was approached from an Fc–PEG–pyrene modified HOPG surface, while the probe oscillation amplitude and current were recorded. The typical amplitude and current approach curves thus obtained (reproduced in ESI,† Fig. S7) allowed a suitable imaging set-point (*i.e.* the imaging distance) to be chosen. The tip was then scanned above the surface while topography and tip current images, such as those presented, respectively, in Fig. 5A and B, were simultaneously acquired.

One can see that, just as above when regular *in situ* AFM was used, the Fc–PEG–pyrene chains were not sensed in topography, the image only shows features typical of the HOPG surface: large atomically flat plateaus separated by steps from $\sim$0.4 nm and up to a few nanometers in height. However one can see from the tip current image in Fig. 5B that the Fc–PEG chains were effectively detected in current. Moreover, the almost uniformly blue color of the current image (ignoring the bottom of the image where the substrate potential was scanned) shows that the Fc–PEG–pyrene chains are *homogenously* distributed all over the HOPG surface. More quantitatively we can conclude that the surface distribution of the Fc–PEG–pyrene chains is homogeneous down to a lateral scale of at least $\sim$20 nm, corresponding to the radius of the tips used here (see ESI†). The dark ''trench'' seen at the bottom of the current image corresponds to a zone where the substrate potential was linearly swept in order to ascertain that the current recorded during imaging is solely ascribable to detection of the Fc–PEG chains by the probe. Such is obviously the case since the i_{tip} *vs.* E_{sub} voltammogram which can be reconstituted from the cross section of the current image displays both the expected S-shape and a mid-height potential value close from the standard potential of the Fc heads, see Fig. 5B (inset). This result also indicates that the electron transfer of the Fc heads at the HOPG substrate is Nernstian, *i.e.* is fast as compared to PEG chain motion. Since the i_{tip} data used to construct the voltammogram shown in Fig. 5B (inset) was mostly sampled at locations clearly corresponding to basal plane regions (as can be ascertained by examining the corresponding topography image), such a finding confirms qualitatively the good electrochemical activity of the basal planes. This falls in line with our previous report describing the AFM-SECM imaging of a HOPG surface using a gold tip functionalized by Fc–PEG chains, and also with a recent report by Unwin *et al.* who used scanning electrochemical cell microscopy (SECCM) to probe the local activity of HOPG.[25] In that respect it is also worth mentioning that we often noticed a very slight variation of the tip current when the tip passed over edge sites of the HOPG surface. Yet, as can be seen from the current cross-section shown in Fig. 5B, this variation was largely lost in the

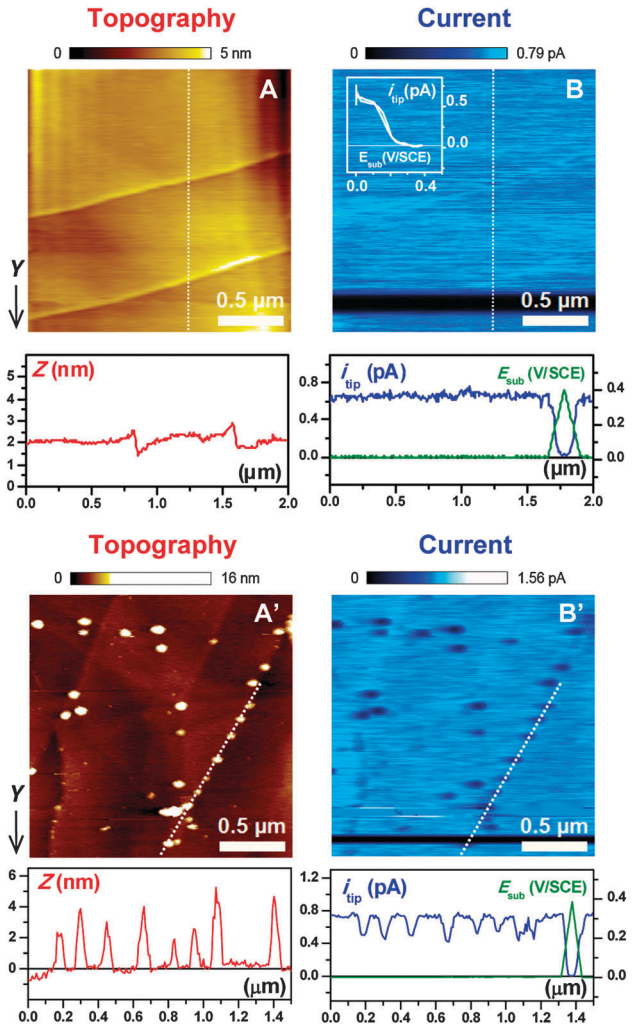

Fig. 5 Tapping mode Mt/AFM-SECM imaging of a HOPG substrate bearing a layer of Fc–PEG–pyrene (Γ = 25 pmol cm^{-2}) before (top) and after deliberate oxidative damaging (bottom). Simultaneously acquired topography (A and A′) and tip current images (B and B′). Cross-sections of the topography and current images taken along the vertical white line shown, passing by some of the nano-objects visible in (A′), are respectively plotted in red and blue below the corresponding images. The images were acquired from top to bottom. In the lower part of the image scan E_{sub} was linearly swept from 0.0 V/SCE to +0.4 V/SCE and back, at 5 mV s^{-1}. This potential sweep is represented by the green trace superimposed onto the current cross-section plot. The inset in (B) is a plot of the tip current, measured along the vertical white line shown in the current images, as a function of the applied substrate potential. The layer was damaged by holding the substrate potential at 0.5 V/SCE for 10 min. The images were acquired using a sharp (~20 nm radius) home-made AFM-SECM probe oscillated at its fundamental flexural frequency = 2.83 kHz. Tip and substrate potentials: E_{tip} = +0.30 V/SCE, E_{sub} = 0.0 V/SCE. Damping ~30%. Imaging rate 0.2 Hz. Aqueous 1 M $NaClO_4$ electrolyte.

current noise. Moreover it sometimes corresponded to a current increase and some other times to a current decrease. Hence we believe these variations to be artefacts containing no reliable information regarding the specific electrochemical activity of edge sites. Another interesting observation we made is that, when the Fc–PEG layer was purposefully damaged *in situ* by prolonged application of a very anodic potential (~0.5 V/SCE) defects appeared in the layer, in the form of seemingly spherically shaped and electro-inactive nano-objects, as shown in Fig. 5A′ and B′ respectively. The nature of these objects is unknown but the mere observation of such nanometer-sized defects, which appear clearly both in the topography and current images, confirms that the initial distribution of Fc–PEG in the intact layer was effectively homogeneous down to the nanometer scale.

The observed homogeneous Fc–PEG–pyrene coverage of these planes shows that the domains (islands, holes) observed in topographic AFM images acquired in air (Fig. 4B and C) only formed upon drying of the layer, and did not pre-exist when the surface was still in solution. Moreover, segregation of the chains into these domains upon drying is a reversible process since we obtained the same images when the surface was first imaged in air and then *in situ* or the other way round. These observations indicate a high degree of mobility of the pyrene foot which allows surface rearrangement of the surface-attached Fc–PEG chains, which is in agreement with recent studies describing the lateral diffusivity of pyrene and other related polycyclic aromatic hydrocarbons adsorbed onto graphene or HOPG surfaces.[23,53]

Conclusions

We have shown, using a multiscale electrochemical approach, that poly(ethylene glycol) (PEG) chains bearing a terminal redox ferrocene (Fc) label head and an anchoring pyrene foot readily self-assemble onto HOPG to form extremely homogeneous layers. However the strongly hydrophobic adsorbing nature of graphite planes results in a complex coverage-dependent structure of the PEG layer due to the interaction of the ferrocene label and the HOPG surface. We showed that below a threshold chain coverage, corresponding to a dimensionless coverage $\sigma^* = \pi R_g^2/s^2 < 1$, chains end-attached to the surface *via* adsorption of the Fc head or the pyrene foot co-exist in the layer. For higher coverage, attachment *via* the pyrene moiety is favoured and the Fc–PEG chains do adopt an ideal "foot-on" end-attached conformation. In this regime we determined that, for the PEG_{3400} chains considered here, the Fc heads are free to explore a volume extending some ~12–14 nm away from the HOPG surface. The results obtained here are likely to be transposable to the case of PEG chains attached to any HOPG-like surface (carbon nanotubes, graphene) *via* a pyrene ring and end-functionalized by a redox, a fluorescent or a binding probe (*e.g.* biotin), all typically displaying some degree of hydrophobicity. Our results suggest that for such probes to efficiently shuttle electrons, fluoresce or undergo molecular recognition – all of these requiring that they are kept away from the graphite surface – the chain coverage should be kept high enough *i.e.* $\sigma^* \geq 1$.

Acknowledgements

This work has benefited from the facilities and expertise of the Small Molecule Mass Spectrometry platform of IMAGIF (Vincent Guerineau, Centre de Recherche de Gif – www.imagif.cnrs.fr).

Notes and references

1 J. M. Harris, in *Poly(Ethylene Glycol) Chemistry: Biotechnical and Biomedical Applications*, ed. J. M. Harris, Plenum Press, New York, 1992.
2 D. Leckband, S. Sheth and A. Halperin, *J. Biomater. Sci., Polym. Ed.*, 1999, **10**, 1125–1147.
3 P. Vermette and L. Meagher, *Colloids Surf., B: Biointerfaces*, 2003, **28**, 153–198.
4 W. P. Wuelfing, S. M. Gross, D. T. Miles and R. W. Murray, *J. Am. Chem. Soc.*, 1998, **120**, 12696–12697.
5 V. Jokers, T. Lobovkina, R. N. Zare and S. S. Gambhir, *Nanomedicine*, 2011, **6**, 715–728.
6 J. Liu, O. Bibari, P. Mailley, J. Dijon, E. Rouvière, F. Sauter-Starace, P. Caillat, F. Vineta and G. Marchanda, *New J. Chem.*, 2009, **33**, 1017–1024.
7 D. Ravelli, D. Merli, E. Quartarone, A. Profumo, P. Mustarellia and M. Fagnoni, *RSC Adv.*, 2013, **3**, 13569–13582.
8 K. S. Novoselov, A. K. Geim, S. V. Morozov, D. Jiang, Y. Zhang, S. V. Dubonos, I. V. Grigorieva and A. A. Firsov, *Science*, 2004, **306**, 666–669.
9 J. H. J. Salavagione, G. Martínez and G. Ellis, *Macromol. Rapid Commun.*, 2011, **32**, 1771–1789.
10 Z. Liu, J. T. Robinson, X. Sun and H. Dai, *J. Am. Chem. Soc.*, 2008, **130**, 10876–10877.
11 L. Q. Xu, W. J. Yang, K.-G. Neoh, E.-T. Kang and G. D. Fu, *Macromolecules*, 2010, **43**, 8336–8339.
12 H. He and C. Gao, *Chem. Mater.*, 2010, **22**, 5054–5064.
13 G. G. F. Schneider, Q. Xu, S. Hage, S. Luik, J. N. H. Spoor, S. Malladi, H. Zandbergen and C. Dekker, *Nat. Commun.*, 2013, **4**, 2619.
14 Y. J. Shin, Y. Wang, H. Huang, G. Kalon, A. Thye Shen Wee, Z. Shen, C. Singh Bhatia and H. Yang, *Langmuir*, 2010, **26**, 3798–3802.
15 J. Israelachvili, *Proc. Natl. Acad. Sci. U. S. A.*, 1997, **94**, 8378–8379.
16 D. Bedrov and G. D. Smith, *Langmuir*, 2006, **22**, 6189–6194.
17 M. Delamar, R. Hitmi, J. Pinson and J.-M. Savéant, *J. Am. Chem. Soc.*, 1992, **114**, 5883–5884.
18 M. Tanaka, T. Sawaguchi, Y. Sato, K. Yoshioka and O. Niwa, *Langmuir*, 2011, **27**, 170–178.
19 C. P. Andrieux, F. Gonzalez and J.-M. Savéant, *J. Am. Chem. Soc.*, 1997, **119**, 4292–4300.
20 C. A. Koval and F. C. Anson, *Anal. Chem.*, 1978, **50**, 223–229.
21 H. Jaegfeldt, T. Kuwana and G. Johansson, *J. Am. Chem. Soc.*, 1983, **105**, 1805–1814.
22 A. A. Gorodetsky and J. K. Barton, *Langmuir*, 2006, **22**, 7917–7922.
23 J. Rodríguez-López, N. L. Ritzert, J. A. Mann, C. Tan, W. R. Dichtel and H. D. Abruña, *J. Am. Chem. Soc.*, 2012, **134**, 6224–6236.
24 R. L. McCreery, *Chem. Rev.*, 2008, **108**, 2646–2687.
25 A. H. Patel, M. Guille Collignon, M. A. O'Connell, W. O. Y. Hung, K. McKelvey, J. V. Macpherson and P. R. Unwin, *J. Am. Chem. Soc.*, 2012, **134**, 20117–20130.
26 K. R. Ward, N. S. Lawrence, R. S. Hartshorne and R. G. Compton, *Phys. Chem. Chem. Phys.*, 2012, **14**, 7264–7275.
27 J. Abbou, A. Anne and C. Demaille, *J. Am. Chem. Soc.*, 2004, **126**, 10095–10108.
28 J. Abbou, A. Anne and C. Demaille, *J. Phys. Chem. B*, 2006, **110**, 22664–22675.
29 A. Anne, E. Cambril, A. Chovin and C. Demaille, *Anal. Chem.*, 2010, **82**, 6353–6362.
30 A. Anne and J. Moiroux, *Macromolecules*, 1999, **32**, 5829–5835.
31 J. V. Macpherson and P. R. Unwin, *Anal. Chem.*, 2000, **72**, 276–285.
32 J. Abbou, C. Demaille, M. Druet and J. Moiroux, *Anal. Chem.*, 2002, **74**, 6355–6363.
33 Y. Zhang, C. Liu, W. Shi, Z. Wang, L. Dai and X. Zhang, *Langmuir*, 2007, **23**, 7911–7915.
34 D. Bléger, F. Mathevet, D. Kreher, A. J. Attias, A. Bocheux, S. Latil, L. Douillard, C. Fiorini-Debuisschert and F. Charra, *Angew. Chem., Int. Ed.*, 2011, **50**, 6562–6566.
35 N. Oyama, K. B. Yap and F. C. Anson, *J. Electroanal. Chem.*, 1979, **100**, 233–246.
36 M. A. G. Zevenbergen, B. L. Wolfrum, E. D. Goluch, P. S. Singh and S. G. Lemay, *J. Am. Chem. Soc.*, 2009, **131**, 11471–11477.
37 S. Alexander, *J. Phys.*, 1977, **38**, 983–987.
38 P. G. de Gennes, *Macromolecules*, 1980, **13**, 1069–1075.
39 E. Karaiskos, I. A. Bitsanis and S. H. Anastasiadis, *J. Polym. Sci., Part B: Polym. Phys.*, 2009, **47**, 2449–2461.
40 J. S. Facci, *Langmuir*, 1987, **3**, 525–530.
41 K. Wang, C. Goyer, A. Anne and C. Demaille, *J. Phys. Chem. B*, 2007, **111**, 6051–6058.
42 H.-J. Butt, B. Cappella and M. Kappl, *Surf. Sci. Rep.*, 2005, **59**, 1–152.
43 S. J. O'Shea, M. E. Welland and T. Rayment, *Langmuir*, 1993, **9**, 1826–1835.
44 H.-J. Butt, M. Kappl, H. Mueller, R. Raiteri, W. Meyer and J. Rühe, *Langmuir*, 1999, **15**, 2559–2565.
45 S. Pasche, M. Textor, L. Meagher, N. D. Spencer and H. J. Griesser, *Langmuir*, 2005, **21**, 6508–6520.
46 J. Israelachvili, *Intermolecular and Surface Forces*, Academic Press, San Diego, 2nd edn, 1992, pp. 288–311.
47 A. K. Dolan and S. F. Edwards, *Proc. R. Soc. London, Ser. A*, 1974, **337**, 509–516.
48 L. Garnier, B. Gauthier-Manuel, E. W. van der Vegte, J. Snijders and G. Hadziioannou, *J. Chem. Phys.*, 2000, **113**, 2497–2503.
49 A. J. Bard, in *Scanning Electrochemical Microscopy*, ed. A. J. Bard and M. V. Mirkin, Marcel Dekker, New York, 2nd edn, 2012, pp. 1–14.
50 M. V. Mirkin, W. Nogala, J. Velmurugan and Y. Wang, *Phys. Chem. Chem. Phys.*, 2011, **13**, 21196–21212.
51 M. Murat and G. S. Grest, *Macromolecules*, 1996, **29**, 8282–8284.
52 V. Koutsos, E. W. Van der Vegte, E. Pelletier, A. Stamouli and G. Hadziioannou, *Macromolecules*, 1997, **30**, 4719–4726.
53 G. Schull, L. Douillard, C. Fiorini-Debuisschert, F. Charra, F. Mathevet, D. Kreher and A. J. Attias, *Nano Lett.*, 2006, **6**, 1360–1363.